Low-cost AUV Swarm Localization Through Multimodal Underwater Acoustic Networks

Federico Mason[‡], Federico Chiariotti[♯], Filippo Campagnaro[‡], Andrea Zanella[‡], Michele Zorzi[‡]

[‡] Department of Information Engineering, University of Padova, via Gradenigo 6/B, 35131 Padova, Italy
[♯] Department of Electronic Systems, Aalborg University, Fredrik Bajers Vej 7, 9220, Aalborg, Denmark.
[‡]{masonfed, campagn1, zanella, zorzi}@dei.unipd.it, [♯]fchi@es.aau.dk

***Abstract*—The use of swarms of Autonomous Underwater Vehicles (AUVs) for environmental monitoring operations could provide important data about pollution, but is currently limited by the high costs of the AUVs and their communication equipment. In this work, we design a system that exploits a multimodal network, composed by both USBL low-frequency and low-cost high frequency acoustic modems, at a much lower cost than standard single mode deployments, and uses distributed sensing and communication-based ranging to perform the localization of an AUV swarm. Our system is able to maintain a positioning error below 13 m over long time periods in different operational scenarios, at a fraction of the cost of the single mode system, and concentrating all the expensive equipment in the leader AUV.**

***Index Terms*—Underwater multimodal networks, Kalman filter, DESERT Underwater, WOSS, Bellhop ray-tracer.**

I. Introduction

Autonomous Underwater Vehicles (AUVs) are submersible underwater nodes able to accomplish a pre-loaded mission with a high level of autonomy. Their missions can cover a large set of applications [1]: scientific underwater exploration, military applications, off-shore industrial applications [2], and applications related to environment protection, like measuring the level of pollution of shipwreck sites. The use of AUVs in these types of missions is very effective compared to human divers in terms of efficiency and risk to human lives.

Military and industrial missions usually involve large scale and expensive AUVs, designed for diving thousands of meters below the sea surface and fully equipped with very sophisticated and expensive tools and sensors, whose prices can easily exceed 1M EUR per unit [3], tailored for specific applications, such as high-resolution 3D scanners [4] and multibeam echosounders [5]. However, applications related to environmental monitoring do not need such expensive equipment as they typically require to inspect the characteristics and the quality of the water column of a large littoral area.

For example, in the case of pollution monitoring, the presence of microplastics in the seawater has been verified up to a depth of 600 m. This kind of monitoring is usually of great interest in coastal waters close to beaches and ports, where the water depth is always less than 100 m. A small and cheap AUV equipped with pollution sensors and communication tools rated for a maximum depth of 200 m, with a price below 50K EUR per unit [6]–[8], can perform the task in a cost-effective manner.

The main challenge is the need to measure the level of pollution in a wide area with high resolution in space and in depth. To accomplish this task, a single AUV would require several sweeps of the area, consuming time and energy. Due to the lack of GPS, the longer the mission of an AUV, the higher its drift from the original path [9]. Therefore, the drawback of this solution is not just the time required to accomplish the mission, but also the low level of spatial resolution due to the position uncertainty. To overcome this issue, a coordinated swarm of N AUVs can be employed to act as a distributed sensor, reducing the duration of the mission by a factor of N and improving the measurement resolution.

AUV formation control and maintenance have been of high interest for the robotics research community in the last years, with a special focus on proposing solutions for Cooperative Navigation (CN), simultaneous localization and mapping (SLAM), and state estimation through extended Kalman filter [10]. In a cooperative navigation system, the AUVs exchange information related to their relative range and direction measurements between each other through an acoustic wireless link [11] in order to improve their localization precision. Several works related to AUV swarm formation [12]–[14] focus on the design and evaluation of the localization and navigation system itself, assuming the existence of a stable and robust acoustic communication link between the AUVs. However, this does not address the significant challenges of the underwater communication channel, such as multipath, low bandwidth, long propagation delay, and the acoustic noise caused by shipping activity and the wind surface waves [15].

In this paper, we analyze the behavior of a leader-follower formation, where the leader is responsible for tracking the followers in order to ensure they are not drifting from the original mission. Specifically, we propose and evaluate two different networks, namely, a single mode low frequency acoustic (`SM`) network, and a low-cost multimodal low frequency and high frequency acoustic network (`MM`). We propose two different communication scenarios for the `MM` network, considering a centralized system (`MM-C`) in which all computation is performed by the leader and the followers just report measurements, as well as a distributed system (`MM-D`) in which the followers implement their own tracking systems and report their state instead of raw measurements.

Part of this work was supported by the US Army Research Office under Grant no. W911NF1910232: "Towards Intelligent Tactical Ad-hoc Networks (TITAN)."

Both the SM and the MM networks are composed of a surface node (e.g., a surface buoy or a vessel) with a well known position, equipped with a GPS receiver and a long range low frequency (LF) acoustic modem, a leader AUV equipped with an LF modem with both normal and inverted ultra-short baseline (USBL) capabilities, and four additional AUVs that act as the followers. In the SM network, all AUVs are equipped with the LF acoustic modem, so the leader can both communicate and track the followers with its USBL LF acoustic modem [16].

SM is currently the most commonly used mode for AUV networks, as it allows each AUV to communicate directly with the surface node and estimate its position with high precision. It relies on commercial off the shelf modems for long range communication [16]–[18] that provide high performance and precision, but have a significant cost, making large AUV formations economically infeasible: prices can easily exceed 8K EUR per acoustic modem (or 16K EUR for a modem with USBL capabilities), with a total communication equipment cost of 16K EUR for the leader and 8K EUR for each follower.

In this paper, we show that it is possible to maintain an acceptable accuracy using the MM network configuration, which requires far cheaper high frequency (HF) acoustic modems. The precision of the localization will be slightly lower, as the HF modems only have ranging capabilities, so only the leader and the surface node can use the LF communication link. The market for high frequency modems includes low-cost acoustic modems which can transmit at a range of a few hundred meters with a bitrate of a few tens to a few hundred bits per second [19], such as the AHOI acoustic modem prototypes developed by the Smartport group of TUHH [20], which have an overall cost of about 600 EUR. We considered the use of the AHOI modems for HF communication in the MM network: in this case, the total cost per follower would be reduced by an order of magnitude.

If we also use low-cost AUV models for the follower units, such as the VENUS AUV developed by ENEA [6], the design would concentrate all the most expensive equipment in the leader unit. In addition to environmental monitoring, this setup can also enable new applications, where, for instance, one of the followers can be elected (or even "sacrificed") for a "high risk task" (e.g., for mine countermeasure or for shipwreck inspection in a harsh environment) with a lower financial risk. Both the SM and MM configurations are presented in Fig. 1.

The rest of this paper is organized as follows: Sec. II describes the system model and the proposed tracking framework in detail, while Sec. III presents the simulation settings and the scenarios we used to verify its performance. The results of the simulation are discussed in Sec. IV, and Sec. V concludes the paper, presenting some avenues of future work.

II. System model

In our model, the performance of network architectures is given by the accuracy with which the leader tracks its own position and those of the followers. To achieve this task, the leader deploys a Bayesian estimator, which requires

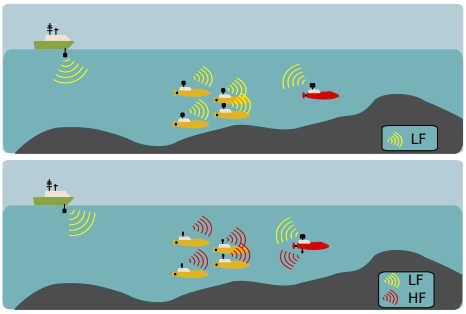

Fig. 1. AUV swarm coordinated with a single mode low frequency acoustic network (above) and with a multimodal low frequency and high frequency acoustic network (below).

knowledge of the evolution of the target state. Hence, the leader assumes that each AUV is in uniform rectilinear motion in the 3D space. We denote node i's position at time t as $\mathbf{x}_i(t) = [x_i(t), y_i(t), z_i(t)]$, and its heading as $\boldsymbol{\psi}_i(t) = [\theta_i(t), \phi_i(t)]$, where $\theta_i(t)$ and $\phi_i(t)$ represent its orientation with respect to the frame of reference on the horizontal and vertical plane, respectively. The motion equations of node i are then given by:

$$\begin{cases} x_i(t+\tau) &= x_i(t) + \cos(\theta_i(t))\cos(\phi_i(t))v_i(t)\tau \\ y_i(t+\tau) &= y_i(t) + \sin(\theta_i(t))\cos(\phi_i(t))v_i(t)\tau \\ z_i(t+\tau) &= z_i(t) + \sin(\phi_i(t))v_i(t)\tau \end{cases}, \quad (1)$$

where $v_i(t)$ is the speed of the considered AUV. We highlight that the motion equations in (1) are a simplified model of the true movements of the target, whose behavior is independent of the tracking system. Finally, we define the state of node i at time t as

$$\mathbf{s}_i(t) = [x_i(t), y_i(t), z_i(t), \theta_i(t), \phi_i(t), v_i(t)], \quad (2)$$

while the network state is given by the union of each different state $\mathbf{s}_i(t)$.

We assume each AUV to be able to measure its current depth using a pressure sensor, as well as its current heading using internal magnetometers and gyroscopes. However, we do not consider independent GPS positioning, as underwater attenuation is too strong to receive the signal from the satellites. Hence, the internal measurement vector for node i at time t is

$$\mathbf{y}_{i,i}(t) = \left[\hat{z}_i(t), \hat{\theta}_i(t), \hat{\phi}_i(t)\right]. \quad (3)$$

We model the measurement error as a multivariate Gaussian random variable with a time-invariant diagonal covariance matrix $\mathbf{R}_{i,i}$, as the measurements come from independent instruments. In both the SM and MM networks, the leader is equipped with a USBL-capable LF modem, which allows to estimate its relative position $\mathbf{x}_{0,1}(t)$ from the ship, which maintains a static position. From now on, we denote the leader as node 1 and the ship as node 0; when it receives a packet from the ship, the leader achieves the following measure:

$$\mathbf{y}_{0,1}(t) = \left[\hat{\mathbf{x}}_{0,1}(t), \hat{\boldsymbol{\psi}}_1(t), \hat{v}_{0,1}(t), \hat{d}_{0,1}(t)\right]. \quad (4)$$

Besides updating its position and heading information, the communication allows the leader to measure two more variables: the Euclidean distance between nodes i and j, i.e., $d_{i,j}(t) = ||\mathbf{x}_i(t) - \mathbf{x}_j(t)||_2$, which is estimated by measuring the round trip time, and the relative speed between nodes i and j, i.e., $v_{i,j}(t) = v_i(t) - v_j(t)$, which is estimated by measuring the Doppler effect. As above, the measurement error is assumed to be a multivariate Gaussian random variable with covariance $\mathbf{R}_{0,1}$.

In our system, the leader also exchanges packets with the follower nodes. Depending on the network configuration, the leader can get the internal measurements of the follower, along with additional information. If the communication between AUVs is low-frequency (SM−C configuration), the leader can get additional information: the LF modem allows the leader to measure the angle of arrival of the signal, as well as the target relative position, resulting in the measurement vector

$$\mathbf{y}_{i,1}^{\text{SM-C}}(t) = \left[\hat{\mathbf{x}}_{i,1}(t), \hat{\boldsymbol{\psi}}_1(t), \hat{v}_{i,1}(t), \hat{d}_{i,1}(t), \hat{z}_i(t), \hat{\boldsymbol{\psi}}_i(t)\right]. \quad (5)$$

Instead, in the MM−C configuration the ranging and Doppler information only allows the leader to estimate the distance between itself and the target and the relative velocity of the latter. Therefore, each time it communicates with a follower with an HF modem, the leader measures the following quantities:

$$\mathbf{y}_{i,1}^{\text{MM-C}}(t) = \left[\hat{v}_{i,1}(t), \hat{d}_{i,1}(t), z_i(t), \hat{\boldsymbol{\psi}}_i(t)\right]. \quad (6)$$

Finally, in the distributed MM−D system, followers implement their own tracking systems, based only on their internal measurements. When they communicate with the leader, follower nodes report the changes in their position as tracked by their internal filter, giving the leader the measurement vector

$$\mathbf{y}_{i,1}^{\text{MM-D}}(t) = \left[\hat{v}_{i,1}(t), \hat{d}_{i,1}(t), \hat{\mathbf{x}}_i(t), \hat{\boldsymbol{\psi}}_i(t)\right]. \quad (7)$$

In all network configurations, we consider a multivariate Gaussian random variable with covariance $\mathbf{R}_{1,i}$ to represent the measurement noise.

In order to estimate the full state of the system $\mathbf{s}(t)$, the leader implements an Unscented Kalman Filter (UKF) [21], which is a widely used tracking algorithm capable of dealing with both linear and non-linear motion models. The update equations for the position of each AUV are given by (1), with an additional zero-mean Gaussian noise with covariance matrix $\mathbf{Q}$. The new information obtained at each time t is variable, and depends on whom the leader communicates with: if it does not communicate during a time step of the filter, its measurement vector coincides with $\mathbf{y}_{1,1}(t)$, while if it communicates with follower i, it is given by a combination of $\mathbf{y}_{1,1}(t)$ and $\mathbf{y}_{i,1}(t)$.

In both the SM and MM networks, the leader retrieves the information from the other nodes in a round-robin fashion. Specifically, it probes each node, one at a time, to receive information about its state, while obtaining ranging information by measuring the round trip time. While in the MM network the leader can only use the USBL modem in inverse mode to estimate its own position when communicating with the surface node, the SM network allows it to use the USBL modem to track each of the followers as well. The MM−D tries to overcome this limitation by improving the self-tracking capabilities of the follower nodes. However, such an implementation entails the transmission of a larger amount of information between AUVs, and, therefore, the leader receives fewer updates.

The MM network presents another issue: the follower nodes have no direct contact with the surface node, so they never get information on their absolute position. This can result in small errors when measuring their heading and speed accumulating over time, resulting in an increasing error as the mission goes on. There are two possible ways to deal with this issue without expensive hardware: the first, and simpler, one, is *off-mission* recalibration: the mission is periodically paused, allowing all AUVs to stop, then send several update messages while moving in a pre-determined pattern. This allows the leader to triangulate the followers' positions and effectively reset the state of the system without additional hardware, but requires more time, as recalibrations can slow down the mission. The second strategy, *on-mission* triangulation, has the AUVs perform triangulation online by using more complex communication topologies. Using a mesh-like topology instead of a star, with communication between followers as well as to the leader, would allow the leader to know the relative distance between follower nodes, triangulating their position and limiting the tracking error. In this work, we consider off-mission recalibration, leaving on-mission triangulation as future work.

III. Simulation settings

In this work, we simulate the SM and MM networks with the multimodal DESERT Underwater protocol stack using the WOSS framework [22], in order to model the acoustic multipath with the Bellhop ray tracer. In all our simulations, a swarm of 5 AUVs moves in an arrowhead formation, with the leader located at the vertex of the arrow. The setup of the SM network is: LF central frequency 25 kHz, bandwidth 5 kHz, datarate 500 bps, and transmission power 175 dB re 1μPa. The round-robin period required for obtaining both USBL data and sensors information from ship and followers has been set to 5.976 s. The MM network uses the same LF modem configuration, and an HF modem with central frequency 50 kHz, bandwidth 25 kHz, datarate 195 bps, and transmission power 156 dB re 1μPa [23].

In the SM−C configuration the LF data period to obtain USBL data from the ship is 3.01 s, while the round-robin period to obtain ranging and sensor data from the followers via HF is 4.26 s for MM−C, and 4.59 s for MM−D. We assume that positions can be quantized using 3 bytes and angles using 2 bytes: this results in a payload of 4 bytes from the followers for the SM−C and MM−C cases (necessary to transmit z, θ and ϕ) and 6 bytes for the MM−D case (as the followers also need to transmit x and y), with a header of 1 byte for each packet. Both the leader and the followers implement a UKF exploiting the Sigma Points parameterization given in [24] and using

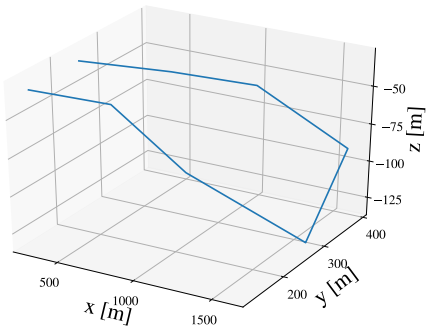

Fig. 2. Path of the *Medium water scenario*.

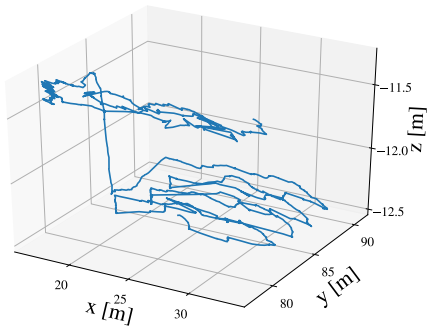

Fig. 3. Path of the *ROV scenario*.

$\alpha = 0.9$, $\beta = 2$ and $\kappa = 10$ as scaling parameters. As process noise we consider $\mathbf{Q} = q\mathbf{I}$, where $\mathbf{I}$ is an identity matrix and $q = 0.01$, while the precision of the system measurements is reported in Table I.

We evaluate the performance of our system in two different deployment scenarios, which are represented in Fig. 2 and Fig. 3. The first is called *Medium water scenario* and emulates the motion of an AUV fleet on a virtual path at a constant speed of 1 m/s with the leader depth varying from 6 to 50 m. In this case, the distance between adjacent AUVs is 54 m: in particular, two followers are deployed 5 m deeper than the leader, while the other two are deployed 10 m deeper than the leader. In this case, packet loss is frequent for communications with the surface node (close to 25%), around 10% for HF communications with followers, and below 1% for LF ones. The Medium water scenario is characterized by linear movements, which should improve the performance of the tracking system, but also has the AUVs move over long distances.

The second scenario considers the real motion of the CNR INM Remotely Operated Vehicle (ROV) described in [25]; for simplicity, we name it *ROV scenario*. During the dive, performed in Biograd Na Moru [26], [27], the ROV was moving between a depth of 1 and 3 meters, at an average speed of 0.2 m/s. In this scenario, the lower distance from the surface vessel reduces the error probability, which is between 5% and 10% for all kinds of communications. Moreover, the distance between adjacent AUVs is 6 m: in particular, two followers are deployed 1 m deeper than the leader, while the other two are deployed 2 m deeper than the leader. In contrast to the Medium water scenario, the ROV scenario is characterized by a lower speed and many turns and changes in direction, as the AUVs are exploring a restricted area.

Measurement	Standard Deviation	Instrument
Depth	0.1 m	Altimeter
Pitch	0.5 °	Inclinometer
Yaw	0.5 °	Magnetometer
Relative speed	0.2 %	Doppler Effect
Relative distance	1 %	Round Trip Time
Relative position	0.5 %	USBL
Yaw, pitch	0.5 °	USBL

TABLE I
MEASUREMENT STANDARD DEVIATIONS.

In both scenarios, we assume that the leader knows the full system state at the beginning of the mission. Moreover, we assume that the AUVs stop the mission at regular intervals to carry out a system recalibration. Such procedure involves a packet exchange between all the system nodes, so that each AUV can estimate its position by a triangulation process. We call *recalibration period* T_c the interval between two consecutive triangulations. The value of T_c should be as large as possible, since a temporary interruption of the mission may negatively affect the AUV task. At the same time, a frequent recalibration of the AUV positions allows the leader to reduce the tracking error.

IV. RESULTS

The system performance is determined by the leader's tracking system, i.e., it coincides with the accuracy of the leader's estimate of its own and its followers' positions. We first consider the Medium water scenario with a simulation period $T_{sim} = 30$ min and a recalibration period $T_c = 20$ min; the obtained results are reported in Fig. 4 and Fig. 5. The first figure shows the boxplot of the tracking error obtained during the *initial stages* of the AUVs' mission, while the latter shows the boxplot of the tracking error obtained during the *advanced stages* of the mission. In particular, we define the initial stage as the first 5 minutes following a system recalibration and the advanced stage as the 5 minute period that precedes a system recalibration. In both figures, we distinguish the leader's self-positioning error from the error on the *close followers* and on the *far followers*, where the close followers are the AUVs moving in the proximity of the leader and the far followers are the AUVs moving at the edges of the arrowhead formation.

We can observe that the self-positioning error remains below 2 m in both Fig. 4 and Fig. 5, as the leader is always able to accurately track its own state thanks to the USBL system. In the `SM-C` configuration, the leader uses the LF modem with USBL to communicate with the followers as well as with the surface node; consequently, the positioning error of both the close and the far followers remains low across the whole mission. In the multi-mode tracking systems, the positioning

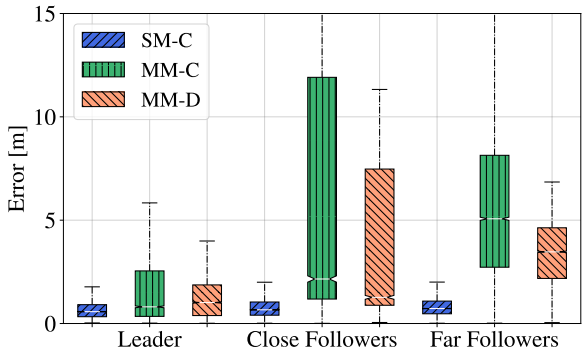

Fig. 4. Medium water scenario, initial stages.

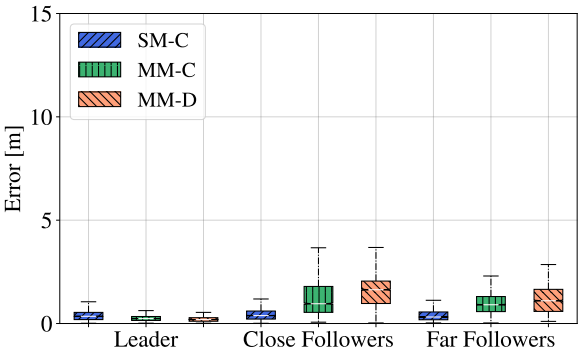

Fig. 6. ROV scenario, initial stages.

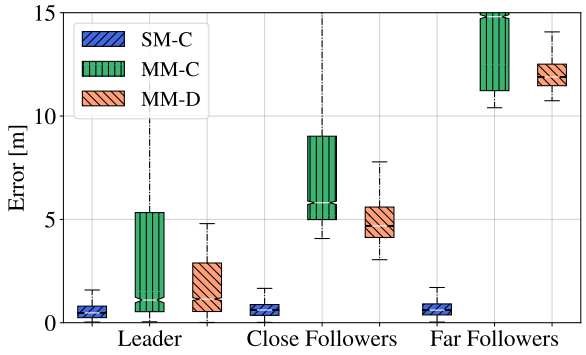

Fig. 5. Medium water scenario, advanced stages.

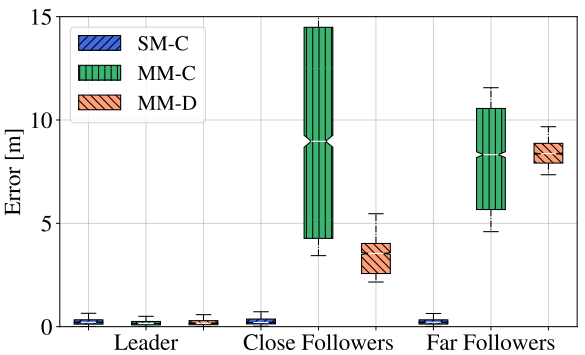

Fig. 7. ROV scenario, advanced stages.

error increases for both the close and the far followers, as MM−C and MM−D do not exploit the USBL system while communicating with the followers. In this case, the position of each AUV is estimated by the communication round trip time, and the tracking performance deteriorates as that distance increases. The main consequence of this is that the positioning error on the far followers is greater than the positioning error on the close followers. We observe that error propagation steadily decreases the estimation accuracy for the followers over time: the system performance in the initial stages are much better in Fig. 4 than in Fig. 5.

In all stages of the mission, the SM−C configuration ensures the best performance; however, as we discussed above, it is also an order of magnitude more expensive, and the performance difference does not justify the expense for applications that do not require high localization precision. Focusing on the other approaches, we observe that the MM−D configuration clearly outperforms the MM−C configuration. The additional Kalman filters installed in the follower AUVs succeed in improving the tracking accuracy despite the longer round trip time due to the larger payload size. Considering a close follower in an advanced stage of the mission, the MM−D system ensures that the 75-th percentile of the positioning error is about 5 m. Under the same conditions, the 75-th percentile of the positioning error obtained with MM−C is about 9 m.

We now focus on the ROV scenario with a simulation period $T_{sim} = 30$ min and a recalibration period $T_c = 20$ min; the obtained results are reported in Fig. 6 and Fig. 7. The SM−C system behaves like in the previous case: the USBL communication allows the leader to accurately track both itself and the followers in all the mission stages. For the same reason, the leader self-positioning error is very low with both MM−C and MM−D; however, if we take the followers into account, the results are different. In both the early stages of the mission, neither of the multi-mode network configurations seems to clearly outperform the other: both MM−C and MM−D ensure a tracking error below about 5 m. Instead, in the mission late stages, the positioning error starts to promptly increase, and MM−D leads to the best results. We can explain this by better analyzing the ROV motion, which is characterized by straight-line movements alternated with sudden turns. This entails that, especially in the mission late stages, it becomes more difficult for the tracking system to estimate the follower positions.

At the beginning of the mission, all the AUVs do not move far away from their starting positions. In this condition, the tracking performance is not affected by the inaccuracy of the local measurements of the followers; the MM−C system performs slightly better, as the leader can receive updates more often. In the advanced stages of the mission, followers move away from their initial positions and the effects of local measurement errors are more significant: as we can observe in

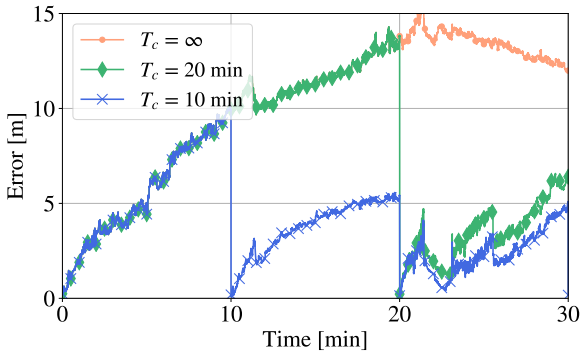

Fig. 8. Medium water scenario.

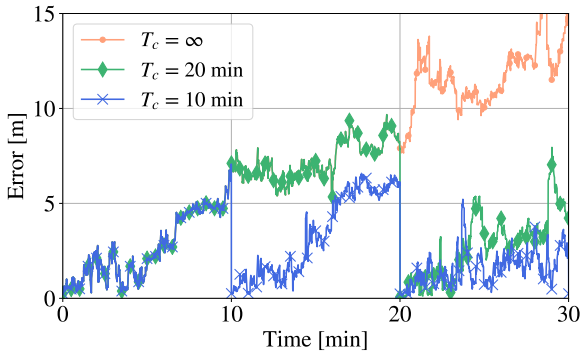

Fig. 9. ROV scenario.

Fig. 7, the MM−D approach becomes more convenient. Considering a close follower in an advanced stage of the mission the 75th percentile of the MM−D tracking error is 10 m lower than the value obtained with the MM−C configuration. Hence, the MM−D network succeeds in keeping the tracking error below 10 m in both the Medium water and ROV scenarios, while the MM−C configuration leads to worse performance.

We conclude our analysis by evaluating the tracking performance of the MM−D network for two different values of the recalibration period T_c; the obtained results are reported in Fig. 8 (for the Medium water scenario) and Fig. 9 (for the ROV scenario), respectively. In particular, we consider three different recalibration schemes: the first exploits a recalibration period of 10 minutes, the second exploits a recalibration period of 20 minutes, while the latter does not carry out any recalibration. As it is intuitive, the shortest recalibration period ensures the best tracking performance, since the target state is repeatedly reset. Conversely, in the configuration without recalibration, the tracking error tends to increase as the simulation goes on.

It is interesting to observe that in Fig. 8 the tracking performance for $T_c = \infty$ is not strictly monotonic: the error reaches its maximum after 20 minutes of simulation and then starts decreasing. We can explain this by analyzing the Medium water path represented in Fig. 2. After 20 minutes of simulations, the AUV fleet is at the maximum depth and the maximum distance from the ship, whose coordinates are (0,0,0). In such a scenario, the packet loss probability increases and, therefore, the tracking system updates its internal state less frequently. When the AUVs move again towards the ship, the communication conditions and the tracking accuracy improve.

V. Conclusions and Future Work

In this work, we have presented a low-cost cooperative multi-mode tracking system for swarms of AUVs that reduces the cost of the communication equipment for the follower nodes by an order of magnitude. If combined with low-cost AUV models, the proposed system can be exploited to make environmental monitoring operations economically viable, solving the cost issue that has slowed the adoption of AUVs in this kind of application. While being less accurate than the more expensive single mode system, our scheme can still achieve an error below 5 m 20 minutes into the mission considering a close follower AUV, and 13 m considering a far follower AUV. A periodic recalibration of the system target state allows to maintain such performance over a longer period.

Future work on the subject includes the development of more advanced communication schemes that can allow larger swarms to maintain formation control with a very limited number of USBL-equipped nodes, using both random access and scheduled strategies. These advanced schemes would remove the need for off-mission recalibration, using multiple subsequent packet exchanges to triangulate the position of all the involved nodes.

References

[1] S. Phoha, E. M. Peluso, and R. L. Culver, "Autonomous underwater vehicles (AUVs): Their past, present and future contributions to the advancement of marine geoscience," *Elsevier Marine Geology*, vol. 352, no. 4, pp. 451–468, Jun. 2014.

[2] G. Ferri, A. Munafo, A. Tesei, P. Braca, F. Meyer, K. Pelekanakis, R. Petroccia, J. Alves, C. Strode, and K. LePage, "Cooperative robotic networks for underwater surveillance: an overview," *IEEE IET Radar, Sonar & Navigation*, vol. 11, no. 1, pp. 1740–1761, August 2017.

[3] "Kongsberg autonomous underwater vehicles," Last time accessed: Aug. 2020. [Online]. Available: https://www.kongsberg.com/maritime/products/marine-robotics/autonomous-underwater-vehicles/

[4] "Kraken seavision," Last time accessed: Aug. 2020. [Online]. Available: https://krakenrobotics.com/products/seavision/

[5] "Kongsberg multibeam echo sounders," Last time accessed: Aug. 2020. [Online]. Available: https://www.kongsberg.com/maritime/products/mapping-systems/mapping-systems/multibeam-echo-sounders/

[6] C. Moriconi, G. Cupertino, S. Betti, and M. Tabacchiera, "Hybrid acoustic/optic communications in underwater swarms," in *Proc. MTS/IEEE OCEANS*, Genova, Italy, May 2015.

[7] "SPARUS II AUV," Last time accessed: Aug. 2020. [Online]. Available: http://iquarobotics.com/sparus-ii-auv

[8] "ecoSUB AUV range," Last time accessed: Aug. 2020. [Online]. Available: https://www.ecosub.uk/ecosubm5---500-m-rated-small-auv.html

[9] A. Munafo, T. Furfaro, G. Ferri, and J. Alves, "Supporting AUV localisation through next generation underwater acoustic networks: results from the field," in *Proc. IEEE/RSJ International Conference on Intelligent Robots and Systems*, Daejeon, Korea, Oct. 2016.

[10] L. Paull, S. Saeedi, M. Seto, and H. Li, "AUV navigation and localization: A review," *IEEE J. Ocean. Eng.*, vol. 39, no. 1, pp. 131–149, Jan. 2014.

[11] Y. Yao, "Cooperative navigation system for multiple unmanned underwater vehicles," in *Proc. IFAC International Conference on Intelligent Control*, Chengdu, China, Sep. 2013.

[12] B. Das, B. Subudhi, and B. B. Pati, "Employing nonlinear observer for formation control of AUVs under communication constraints," *International Journal of Intelligent Unmanned Systems*, vol. 3, no. 2, pp. 122–155, May 2015.

[13] P. Millan, L. Orihuela, I. Jurado, and F. R. Rubio, "Formation Control of Autonomous Underwater Vehicles Subject to Communication Delays," *IEEE Transactions on Control Systems Technology*, vol. 22, no. 2, pp. 770–777, March 2014.

[14] Z. Hu, C. Ma, L. Zhang, A. Halme, T. Hayat, and B. Ahmad, "Formation Control of Autonomous Underwater Vehicles Subject to Communication Delays," *ELSEVIER Neurocomputing*, vol. 147, no. 5, pp. 291–298, January 2015.

[15] M. Stojanovic, "On the relationship between capacity and distance in an underwater acoustic communication channel," *ACM Mobile Comput. and Commun. Review*, vol. 11, no. 4, pp. 34–43, Oct. 2007.

[16] "EvoLogics Underwater Acoustic Modems," Last time accessed: Aug. 2020. [Online]. Available: https://evologics.de/acoustic-modems

[17] "Develogic Subsea Systems," Last time accessed: Aug. 2020. [Online]. Available: http://www.develogic.de/

[18] "Teledyne-benthos acoustic modems," accessed: March 2020. [Online]. Available: http://www.teledynemarine.com/acoustic-modems/

[19] "WATER LINKED Modem M64," Last time accessed: Aug. 2020. [Online]. Available: https://waterlinked.com/product/modem-m64/

[20] B.-C. Renner, J. Heitmann, and F. Steinmetz, "AHOI: Inexpensive, low-power communication and localization for underwater sensor networks and μAUVs," *ACM Transactions on Sensor Networks*, vol. 16, no. 2, pp. 251–273, Jan. 2020.

[21] E. A. Wan and R. Van Der Merwe, "The unscented Kalman filter for nonlinear estimation," in *Proceedings of the IEEE 2000 Adaptive Systems for Signal Processing, Communications, and Control Symposium (Cat. No. 00EX373)*. IEEE, 2000, pp. 153–158.

[22] F. Campagnaro, R. Francescon, F. Guerra, F. Favaro, P. Casari, R. Diamant, and M. Zorzi, "The DESERT underwater framework v2: Improved capabilities and extension tools," in *Proc. Ucomms*, Lerici, Italy, Sep. 2016.

[23] A. Signori, F. Campagnaro, F. Steinmetz, B.-C. Renner, and M. Zorzi, "Data gathering from a multimodal dense underwater acoustic sensor network deployed in shallow fresh water scenarios," *MDPI Journal of Sensor and Actuator Networks*, vol. 8, no. 4, Nov. 2019.

[24] R. V. D. Merwe, "Sigma-point Kalman filters for probabilistic inference in dynamic state-space models," Ph.D. dissertation, OGI School of Science & Engineering at OHSU, 2004.

[25] A. Odetti, M. Bibuli, G. Bruzzone, M. Caccia, E. Spirandelli, and G. Bruzzone, "e-URoPe: a reconfgurable AUV/ROV for man-robot underwater cooperation," *IFAC-PapersOnLine*, vol. 50, no. 1, pp. 11 203–11 208, 2017.

[26] R. Ferretti, M. Bibuli, M. Caccia, D. Chiarella, A. Odetti, E. Zereik, and G. Bruzzone, "Towards posidonia meadows detection, mapping and automatic recognition using unmanned marine vehicles," *IFAC-PapersOnLine*, vol. 50, no. 1, pp. 12 386–12 391, 2017.

[27] M. Bibuli, E. Zereik, G. Bruzzone, M. Caccia, R. Ferretti, and A. Odetti, "Practical experience towards robust underwater navigation," *IFAC-PapersOnLine*, vol. 51, no. 29, pp. 281–286, 2018.